

# Longitudinal sound velocity and internal friction in ferromagnetic $\text{La}_{1-x}\text{Sr}_x\text{MnO}_3$ single-crystal manganites

R. I. Zainullina, N. G. Bebenin, A. M. Burkhanov, and V. V. Ustinov

*Institute of Metal Physics, Ural Division of RAS, Kovalevskaya Str. 18, Ekaterinburg 620219, Russia*

Ya. M. Mukovskii

*Moscow State Steel & Alloys Institute, Leninskii Prosp., 4, Moscow 117936, Russia*

(Received 4 February 2002; revised manuscript received 29 April 2002; published 16 August 2002)

We have studied the temperature dependence of sound velocity and internal friction in ferromagnetic  $\text{La}_{1-x}\text{Sr}_x\text{MnO}_3$  single crystals,  $x=0.15, 0.20$ , and  $0.25$ , grown by the floating zone method. The sound velocity and internal friction were determined by the composite oscillator method at frequencies of order 100 kHz. The compositional metal-insulator transition has been found to be accompanied by an increase of the sound velocity and a weakening of its temperature dependence. It is likely that  $\text{La}_{0.85}\text{Sr}_{0.15}\text{MnO}_3$  undergoes a transition between the  $O^*$  phase and an unknown phase at about 60 K. In  $\text{La}_{0.80}\text{Sr}_{0.20}\text{MnO}_3$ , a weak transition of the first order occurs at 400 K. It has been revealed that the giant thermal hysteresis of sound velocity and internal friction is the specific feature of the  $Pnma$ - $R\bar{3}c$  transition; therefore, in a wide temperature range there is the mixture of these crystalline phases. Above 400 K, relaxation peaks of the internal friction due to point defects have been found.

DOI: 10.1103/PhysRevB.66.064421

PACS number(s): 75.30.Vn, 62.30.+d, 62.40.+i

## I. INTRODUCTION

The interest in lanthanum manganites  $\text{La}_{1-x}D_x\text{MnO}_3$ , with  $D$  being a divalent ion (Ca, Sr, Ba, or Pb), as well as in the manganites of other rare earths is stimulated by the colossal magnetoresistance (CMR) effect that is observed near the Curie temperature  $T_C$ .<sup>1-5</sup> The characteristic feature of the CMR manganites is the strong interaction between charge carriers in the  $e_g$  band, localized spins of  $t_{2g}$  electrons, and the crystal lattice. As a result, the manganites undergo magnetic phase transitions, structural transformations, charge ordering, and a metal-insulator transition. Although the role of the lattice in forming the properties of the CMR compounds is universally recognized, the lattice properties as such remain weakly investigated. The publications on sound propagation in these oxides<sup>6-13</sup> are not numerous, and only some of them contain information on sound damping. There are a few papers dealing with the evolution of the elastic moduli with the divalent ion concentration<sup>7,10</sup> but the change of the damping with  $x$  seems not to be studied yet. The interpretation of the experimental results<sup>10</sup> was made in the frame of the ionic picture and based on the supposition that the temperature dependence of the moduli is due to the Jahn-Teller (JT) effect only.

In this paper, we report on a systematic study of the temperature dependence of longitudinal sound velocity  $V_1$  and internal friction  $Q^{-1}$  in  $\text{La}_{1-x}\text{Sr}_x\text{MnO}_3$  single crystals with  $x=0.15, 0.20$ , and  $0.25$  in the temperature range of 6–425 K; the magnetization was also measured. If  $x < 0.25$ , a manganite of this family is in the orthorhombic phase of  $Pnma$  symmetry at low temperature, while the high-temperature phase is a rhombohedral phase of the  $R\bar{3}c$  space group.<sup>14</sup> Doping reduces the temperature  $T_S$  of the  $Pnma$ - $R\bar{3}c$  transformation, and manganites with  $x$  greater than 0.25 are allways in the rhombohedral phase. Kawano *et al.*<sup>15</sup> have revealed

that in fact there are two orthorhombic phases of the  $Pnma$  symmetry: an  $O'$  phase with strong JT distortions and a pseudocubic  $O^*$  phase in which the JT distortions are absent. No different rhombohedral phases have been reported so far.

Yamada *et al.*<sup>16</sup> observed a low-temperature charge-ordering (CO) state in the crystals with  $x$  around 0.125; in particular  $\text{La}_{0.85}\text{Sr}_{0.15}\text{MnO}_3$  was found to undergo the transition into the CO state approximately at 200 K. The Curie temperature  $T_C$  of all the samples studied as well as  $T_S$  and  $T_{CO}$  are within our temperature range of 6–425 K, so that it is possible to compare the effect of transitions of different types on the elastic properties. The  $x=0.15$  crystal is an insulator at any temperature while the  $x=0.20$  and  $0.25$  manganites are insulators in a paramagnetic state only, exhibiting metallic behavior in a ferromagnetic state.<sup>14</sup> Therefore we can also estimate how the elastic properties are influenced by the metal-insulator transition. We pay special attention to the temperature hysteresis of  $V_1$  and  $Q^{-1}$ , and show that the boundary between  $Pnma$  and  $R\bar{3}c$  phases is fuzzy in the sense that the phases coexist in a very broad temperature interval.

Also we have observed anomalies that cannot be attributed to the known transitions. The analysis shows that some of the anomalies result from structural transitions not observed earlier and others are due to a relaxation process.

## II. EXPERIMENT

The  $\text{La}_{1-x}\text{Sr}_x\text{MnO}_3$  single crystals were grown by the floating-zone method; the details have been published earlier.<sup>17</sup> The as-grown samples used in our ultrasound experiments were cylinders of about 30 mm long and 3 mm in diameter. The cylinder axis was along the cubic  $[103]$  direction in the  $x=0.15$  sample, along  $[111]$  in the  $x=0.20$  crystal, and along  $[115]$  in the  $x=0.25$  sample.

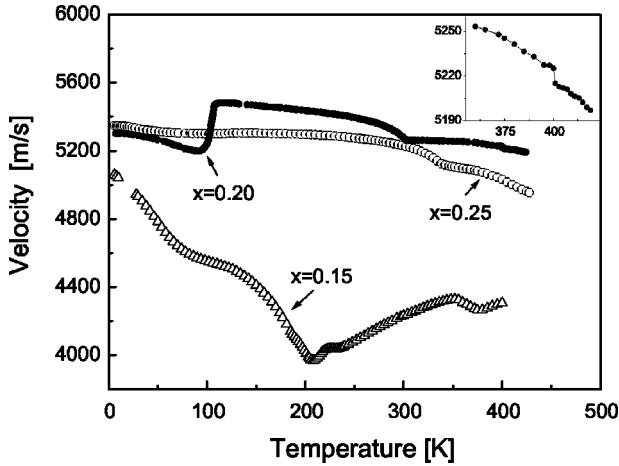


FIG. 1. Temperature dependence of the sound velocity of  $\text{La}_{1-x}\text{Sr}_x\text{MnO}_3$  single crystals measured at warming. Inset: the sound velocity of the  $x=0.20$  crystal near  $T'_S$  (the final curve after eight “warming-cooling” cycles).

The sound velocity and internal friction were determined by the composite oscillator method.<sup>18</sup> The resonance frequency and quality of the mechanical system consisting of a manganite sample and a quartz rod exciting longitudinal vibrations were measured, and then  $V_1$  and  $Q^{-1}$  were calculated for the manganite. The frequency was of order 100 kHz. The measurements were carried out in helium gas atmosphere under warming and cooling with the rate of 15–30 K per hour. The vibrating sample magnetometer was used for measuring magnetization.

### III. RESULTS OF MEASUREMENTS

The magnetization curves of the manganites studied are typical for a ferromagnet. The Curie temperatures determined through Arrot-Belov curves are 232, 308, and 341 K for the  $x=0.15$ , 0.20, and 0.25 samples, respectively, which are very close to the values reported by Urushibara *et al.*<sup>14</sup> The value of the resistivity and its temperature dependence are also quite similar to that observed by the authors of Ref. 14.

Figure 1 shows the temperature dependence of  $V_1$  taken at warming. The  $\text{La}_{0.85}\text{Sr}_{0.15}\text{MnO}_3$  manganite stands out owing to the large change of  $V_1$  with  $T$ . On the curve for the  $x=0.15$  sample, one can see the following anomalies: the deep minimum at 208 K related to the charge ordering, the weak minimum at 230 K due to a transition from a ferromagnetic state to a paramagnetic state, and the minimum at 377 K due to the  $Pnma-R\bar{3}c$  transformation. Below  $T_{CO}$ , the sound velocity strongly decreases with growing  $T$ , but in the range from 50 to 100 K the derivate  $dV_1/dT$  is small. Besides the main resonance, we observed an addition resonance in the interval of 180–240 K, which is likely to be due to inhomogeneity of the  $x=0.15$  manganite, as discussed in Ref. 12.

The increase of the strontium content results in an increase of the value and in a weakening of the temperature dependence of the sound velocity. The Curie temperature

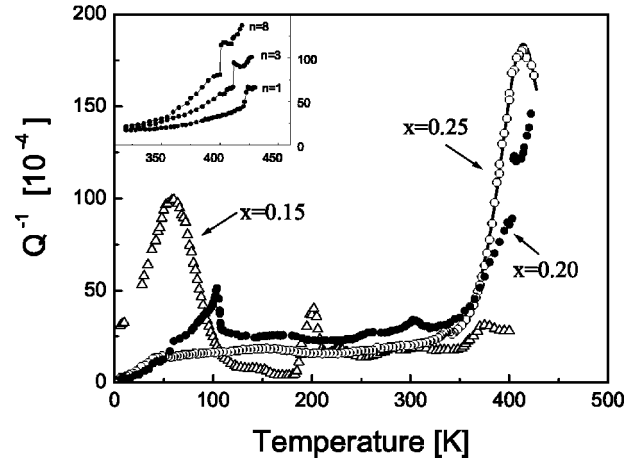


FIG. 2. Temperature dependence of internal friction  $Q^{-1}$  of  $\text{La}_{1-x}\text{Sr}_x\text{MnO}_3$  single crystals measured at warming. The solid line is the calculated curve by Eq. 2 with an activation energy of  $H=0.65$  eV. Inset:  $Q^{-1}(T)$  near  $T'_S$  in  $\text{La}_{0.80}\text{Sr}_{0.20}\text{MnO}_3$ ;  $n$  is the number of “warming-cooling” cycles.

manifests itself as a break on the  $V_1$ - $T$  curves. On the curve for the  $\text{La}_{0.80}\text{Sr}_{0.20}\text{MnO}_3$ , there is a discontinuity at 104 K caused by the structural  $Pnma-R\bar{3}c$  transformation. There is also another weak jump in  $V_1$  at  $T'_S=400$  K; see the inset in Fig. 1, which indicates a first-order transition. This transition was not observed earlier. In the  $x=0.25$  compound, the sound velocity decreases monotonically with increasing temperature.

Figure 2 shows the temperature dependence of the internal friction  $Q^{-1}$  measured under warming. On the curve for the  $x=0.15$  crystal, one can see the peaks at 60, 202, 227, and 375 K. The last three maxima are obviously due to the charge ordering, the Curie point, and the  $Pnma-R\bar{3}c$  transformation, respectively. The peak at 60 K is likely to be due to the transition between orthorhombic  $O^*$  phase and an unknown low-temperature phase; see Sec. IV.

On the  $Q^{-1}$ - $T$  curve for the  $x=0.20$  manganite, there is a maximum at 104 K caused by the  $Pnma-R\bar{3}c$  transformation and another weak maximum at 302 K due to the transition from a ferromagnetic state to a paramagnetic state. When  $T>360$  K, there is a strong increase of the internal friction with the jump at temperature of 400 K. This jump seems to be due to superposition of a sharp peak centered at  $T'_S$  and a monotonic curve.

The  $Q^{-1}$ - $T$  curve for the  $x=0.25$  crystal exhibits no anomaly below the Curie temperature, and has a weak maximum near  $T_C$ . A further increase of temperature results in the strong increase of the internal friction, which reaches a maximum at 415 K.

Since the  $Pnma-R\bar{3}c$  transition is of first order, the thermal hysteresis has to be observed. Figure 3 shows the hysteretic behavior of the magnetization  $M$  in  $\text{La}_{0.80}\text{Sr}_{0.20}\text{MnO}_3$ . The transition temperature can be conveniently defined as a half-sum of the temperatures corresponding to the maximum slopes of the curves  $M(T)$  recorded in the cooling and warming; we then obtain  $T_S=95$  K. The noticeable ampli-

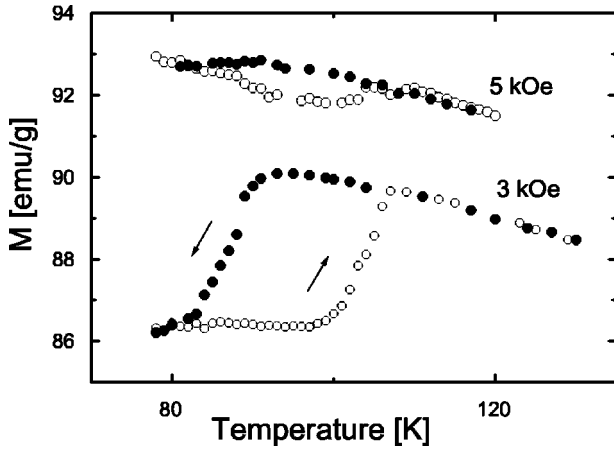


FIG. 3. Magnetization of  $\text{La}_{0.80}\text{Sr}_{0.20}\text{MnO}_3$  in the vicinity of the  $Pnma-R\bar{3}c$  transition.

tude of the thermal hysteresis loop observed in the region of technical magnetization ( $H=3$  kOe) points to the change of the magnetic anisotropy under the  $Pnma-R\bar{3}c$  transformation. In the true magnetization region ( $H=5$  kOe) the difference in the magnetization values is only about 0.7 emu/g. The width of the thermal hysteresis loop is independent of  $H$  and approximately equal to 25 K. No thermal hysteresis in magnetization was observed in  $\text{La}_{0.85}\text{Sr}_{0.15}\text{MnO}_3$  or  $\text{La}_{0.75}\text{Sr}_{0.25}\text{MnO}_3$ .

Let us turn to the elastic properties. The temperature dependence of  $V_1$  and  $Q^{-1}$  for  $\text{La}_{0.80}\text{Sr}_{0.20}\text{MnO}_3$  displays pronounced hysteretic behavior connected with the structural  $Pnma-R\bar{3}c$  transformation. Figures 4 and 5 show that the hysteresis of elastic properties takes place in the range of 50–350 K, so that the width of the hysteresis loop (300 K) is giant as compared with the  $T_S$ . The loop is asymmetrical: its extent to higher temperatures (about 250 K) is much greater than down to lower temperatures (about 50 K). Similar hysteresis has been observed in the  $x=0.15$  crystal in the range of 200–425 K. The curves  $V_1(T)$  and  $Q^{-1}(T)$  for the  $\text{La}_{0.75}\text{Sr}_{0.25}\text{MnO}_3$  measured under warming and cooling practically coincide.

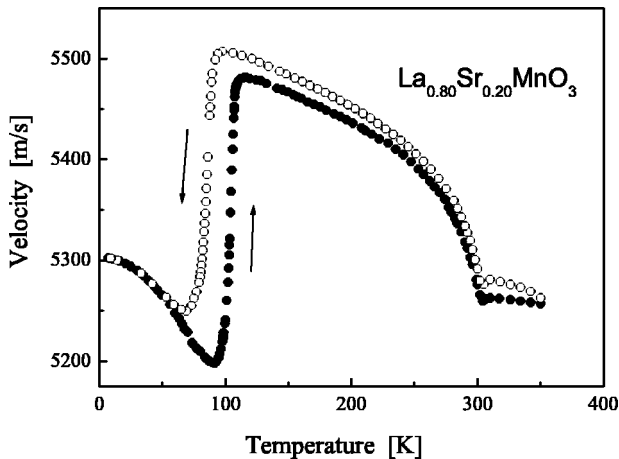


FIG. 4. Giant thermal hysteresis of the sound velocity in a  $\text{La}_{0.80}\text{Sr}_{0.20}\text{MnO}_3$  single crystal.

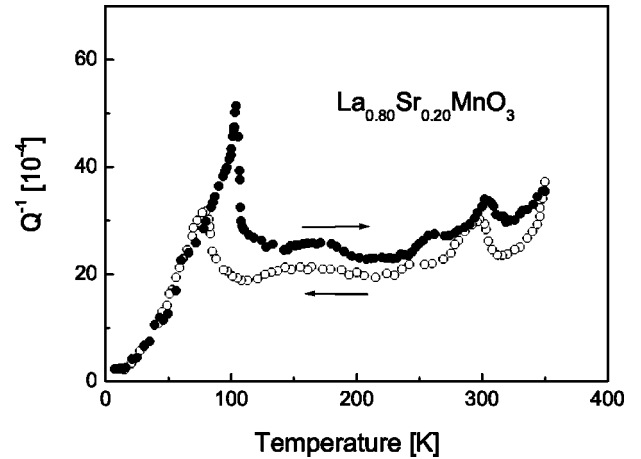


FIG. 5. Hysteretic behavior of internal friction in a  $\text{La}_{0.80}\text{Sr}_{0.20}\text{MnO}_3$  single crystal.

The temperature hysteresis was also observed in the vicinity of  $T'_S$ , but  $T'_S$  and the width of the loop turned out to depend on the prehistory of the sample, specifically on the number  $n$  of “warming-cooling” cycles in the range of 300–430 K. After eight cycles,  $T'_S$  was reduced from 420 to 400 K and the width was decreased from 8 K to a value less than 1 K; no further ( $n>8$ ) change of  $T'_S$  was observed. The inset to Fig. 2 shows the reduction of  $T'_S$  and the increase of  $Q^{-1}$  with  $n$ . The value of the jump in  $V_1$  did not depend on  $n$  and is very small, as follows from the final  $V_1$ - $T$  curve in the inset to Fig. 1.

#### IV. DISCUSSION

The sound velocity  $V_1$  in a cylinder is determined by the Young’s modulus  $E$ :  $V_1 = \sqrt{E/\rho}$ , with  $\rho$  being a density. In a single crystal, the Young’s modulus depends on the orientation of the cylinder axis relative to crystal axes. For the cubic symmetry one can write<sup>19</sup>

$$\frac{1}{E} = \frac{c_{11} + c_{12}}{(c_{11} + 2c_{12})(c_{11} - c_{12})} + \left( \frac{1}{c_{44}} - \frac{2}{c_{11} - c_{12}} \right) P(\mathbf{n}), \quad (1)$$

where  $P(\mathbf{n}) = n_x^2 n_y^2 + n_x^2 n_z^2 + n_y^2 n_z^2$ , and  $\mathbf{n}$  is a unit vector along the cylinder axis. It has been reported in Ref. 10 that in  $\text{La}_{0.835}\text{Sr}_{0.165}\text{MnO}_3$  single crystal,  $c_{11} = 12.7 \times 10^{11}$  erg/cm<sup>3</sup>,  $(c_{11} - c_{12})/2 = 4.5 \times 10^{11}$  erg/cm<sup>3</sup>,  $c_{44} = 5.4 \times 10^{11}$  erg/cm<sup>3</sup> at  $T = 200$  K, so that  $E = [0.0907 - 0.037P(\mathbf{n})]^{-1} \times 10^{11}$  erg/cm<sup>3</sup>. Since  $P(\mathbf{n})$  cannot be greater than 1/3, we infer that the elastic anisotropy of  $\text{La}_{0.835}\text{Sr}_{0.165}\text{MnO}_3$  is rather weak. Assuming this to be true for every ferromagnetic crystal of the  $\text{La}_{1-x}\text{Sr}_x\text{MnO}_3$  family, we conclude that our experiments give information on the first term in Eq. (1);  $c_{44}$  as well as the dependence on  $\mathbf{n}$  is of minor importance.

#### A. Compositional metal-insulator transition and elastic moduli

We have already seen that an increase of the Sr content leads to an increase in  $V_1$ , and that the temperature dependence of  $V_1$  is essentially stronger in the  $x=0.15$  crystal than in the  $x=0.20$  and 0.25 ones. Similar changes have been

reported in Ref. 10 for  $\text{La}_{0.835}\text{Sr}_{0.165}\text{MnO}_3$  and  $\text{La}_{0.7}\text{Sr}_{0.3}\text{MnO}_3$  single crystals. This difference cannot be attributed to the change of the lattice symmetry, because below 90 K the values of the sound velocity in the  $x=0.20$  and 0.25 samples are very close to each other (see Fig. 1), although  $\text{La}_{0.80}\text{Sr}_{0.20}\text{MnO}_3$  is in the orthorhombic phase while  $\text{La}_{0.75}\text{Sr}_{0.25}\text{MnO}_3$  is in the rhombohedral one. Therefore, we tentatively ascribe the change in temperature dependence of  $V_1$  to the compositional metal-insulator transition. Unfortunately we are not able to justify this supposition by a comparison with theory, since a theory explaining how metal-insulator transition influences the elastic moduli is seemingly absent.

### B. Phase transitions

The anomalies observed on  $V_1$ - $T$  and  $Q^{-1}$ - $T$  curves agree with the positions of the magnetic and structural transitions published earlier. Let us first consider  $\text{La}_{0.85}\text{Sr}_{0.15}\text{MnO}_3$ . There is a maximum of the internal friction at 375 K (Fig. 2) when the transition occurs between the high-temperature rhombohedral and orthorhombic  $Pnma$  crystal structures with parameters  $a=5.546$  Å,  $b/\sqrt{2}=5.504$  Å, and  $c=5.518$  Å ( $T=300$  K). Estimating Mn-O distances at 300 K indicates JT distortions and hence an  $O'$  phase. The maximum of  $Q^{-1}$  at the magnetic phase transition is weak; therefore, no structural transformation occurs at the Curie point. At around 200 K, charge ordering takes place.<sup>16</sup> Vasiliu-Doloc *et al.*<sup>20</sup> observed a transition from an  $O'$  phase to a  $O^*$  phase in the  $x=0.15$  manganite at about 200 K. Therefore the charge ordering is accompanied by the  $O'-O^*$  transition which explains the sharp maximum of  $Q^{-1}$ .

The strong peak of the internal friction is seen at  $T=60$  K, i.e., well below the point of the  $O'-O^*$  transition. Low-temperature peaks are observed in some metals where they are explained by the dislocation relaxation.<sup>21</sup> However this mechanism is unlikely to be realized in our case because the peak is completely absent in the  $x=0.20$  and 0.25 samples produced by the same method. We assume that the peak at  $T=60$  K is caused by the transition from the pseudocubic  $O^*$  phase to an unknown phase; in samples with greater Sr content this transition is absent. Our assumption is supported by the fact that in the range of 15–60 K, the thermal expansion in  $\text{La}_{0.85}\text{Sr}_{0.15}\text{MnO}_3$  exhibits a strong anomaly, which is similar to the anomalies caused by  $Pnma$ - $R\bar{3}c$  or  $O'-O^*$  transitions.<sup>12</sup> The transition between  $O^*$  and the unknown phase is fuzzy (the peak width is about 55 K), so that, even at  $T=6$  K, there is a mixture of the two crystal phases, which gives rise to the strong internal friction.

Now we turn to the first order transition at  $T'_S=400$  K in  $\text{La}_{0.80}\text{Sr}_{0.20}\text{MnO}_3$ . The jump in  $V_1$  at  $T'_S$  is an order of magnitude less than that at  $T_S$ , which points to a weak change of the crystal lattice during this transition. Perhaps the space group does not change; in other words, this is a transition between two phases that belong to one and the same  $R\bar{3}c$  structure. The observed dependence of the transition temperature and the hysteresis loop width on the number of the “warming-cooling” cycles may be attributed to the relax-

ation of the internal stress that was induced during the growth of the single crystal. Indeed, the relaxation happens through the formation of defects that can play a role of nucleation centers. Decreasing the stress leads to a change in  $T'_S$ , while the growth of the number of centers results in a decrease of the loop width and an increase of the sound damping.

### C. Giant thermal hysteresis

The anomalies connected with the  $Pnma$ - $R\bar{3}c$  transformation is distinct for the  $x=0.20$  sample. The giant width of the thermal hysteresis loop indicates that under warming from a temperature well below 104 K, the regions of the  $Pnma$  phase exist up to 350 K. Above  $T_S$ , the value of  $Q^{-1}$  (at a given temperature) is greater if the sample is heated from liquid helium temperature than under cooling from a temperature in the paramagnetic region. Therefore, under warming from  $T < T_S$ , there are additional centers of scattering of sound waves up to 350 K, which confirms the existence of the  $Pnma$  inclusions in an  $R\bar{3}c$  matrix up to 350 K. When cooling from 350 K, the  $Pnma$  inclusions are absent down to a close vicinity of  $T_S$ .

Using the data of Fig. 4, we can roughly estimate the relative volume  $\epsilon$  of orthorhombic inclusions in the rhombohedral matrix at  $T > T_S$ . Assuming  $V_1 = V_1^{\text{rhom}}(1-\epsilon) + V_1^{\text{ortho}}\epsilon$  and taking the difference  $V_1^{\text{rhom}} - V_1^{\text{ortho}} = 260$  m/s not to depend on  $T$ , we find  $\epsilon \approx 0.06$  at  $T=200$  K. Thus, even at a temperature much greater than  $T_S$ , the orthorhombic inclusions still occupy some percent of the sample volume.

### D. Point defects

The anomaly at 400 K on the  $Q^{-1}$ - $T$  curve for  $\text{La}_{0.80}\text{Sr}_{0.20}\text{MnO}_3$  is observed on the background of the intense growth of the internal friction. Comparison with the curve for  $\text{La}_{0.75}\text{Sr}_{0.25}\text{MnO}_3$  shows that in both samples we deal with a strong peak of  $Q^{-1}$ , but in the  $x=0.20$  crystal the peak is beyond the temperature region in which the measurements were carried out. Similar maximum at temperature of 395 K was found earlier in  $\text{La}_{0.60}\text{Eu}_{0.07}\text{Sr}_{0.33}\text{MnO}_3$ .<sup>9</sup> The increase of the Sr content reduces the peak temperature. Such a reduction is, however, not large. Therefore these peaks of the internal friction are unlikely to be due to a structural transformation, since in the CMR manganites, the structural transition temperatures strongly depend on the divalent ion content. We may thus suppose that the peaks can be explained by a relaxation process. In this case,

$$Q^{-1} \propto \frac{\omega\tau}{1 + (\omega\tau)^2}, \quad (2)$$

where  $\omega$  is the frequency,  $\tau = \tau_o \exp(H/k_B T)$ ,  $\tau_o$  is a constant, and  $H$  stands for the activation energy. Using formula (2), we have treated the high-temperature peaks of the internal friction and found  $H$  for the  $\text{La}_{0.75}\text{Sr}_{0.25}\text{MnO}_3$  single crystal and the  $\text{La}_{0.60}\text{Eu}_{0.07}\text{Sr}_{0.33}\text{MnO}_3$  polycrystal. The activation energy turns out to be the same for both samples:  $H=0.65$  eV. One can see in Fig. 2 (solid line) that the peak on the  $x=0.25$

curve is well fitted with expression (2). An activation energy of 0.1–1.0 eV is characteristic of point defects.<sup>22</sup> Taking into account the high content of divalent ions and the tendency toward vacancy formation, we may suggest that the peaks are due to the complexes of point defects involving vacancies. It is worth noting that the optical absorption caused by the transitions between energy levels of clusters formed by manganese and oxygen has already been reported, see, e.g., Ref. 23.

## V. CONCLUSION

We have studied the temperature dependence of the sound velocity and internal friction in ferromagnetic  $\text{La}_{1-x}\text{Sr}_x\text{MnO}_3$  single crystals. The compositional metal-insulator transition has been found to be accompanied by the increase of the sound velocity and weakening its temperature dependence. Such a behavior can be explained by interactions of the lattice with the charge carriers in the  $e_g$  band, which are absent at  $T < T_C$  in  $\text{La}_{0.85}\text{Sr}_{0.15}\text{MnO}_3$  but present in  $\text{La}_{0.80}\text{Sr}_{0.20}\text{MnO}_3$  and  $\text{La}_{0.75}\text{Sr}_{0.25}\text{MnO}_3$ .

Our experiments have revealed the anomalies that can be caused by phase transitions not observed earlier, to our knowledge. It is likely that in  $\text{La}_{0.85}\text{Sr}_{0.15}\text{MnO}_3$ , the transition between the  $O^*$  phase and an unknown phase occurs at about 60 K. In  $\text{La}_{0.80}\text{Sr}_{0.20}\text{MnO}_3$ , the first order structural transition, at which the change of the sound velocity is much less than during the  $Pnma-R\bar{3}c$  structural transformation, takes place at 400 K, which indicates that there two different rhombohedral phases.

The giant thermal hysteresis of the sound velocity and internal friction has been found to be a specific feature of the  $Pnma-R\bar{3}c$  transition. This means that in the CMR manganites, the boundary between the crystal phases is fuzzy. Above 400 K, the relaxation peaks of the internal friction due to point defects have been found.

## ACKNOWLEDGMENTS

We are grateful to V.S. Gaviko for x-ray measurements. The work was supported by RFBR Grant Nos. 00-02-17544 and 00-15-96745.

- 
- <sup>1</sup>Y. Tokura and Y. Tomioka, *J. Magn. Magn. Mater.* **200**, 1 (1999).  
<sup>2</sup>J.M.D. Coey, M. Viret, and S. von Molnar, *Adv. Phys.* **48**, 167 (1999).  
<sup>3</sup>E. Dagotto, T. Hotta, and A. Moreo, *Phys. Rep.* **344**, 1 (2001).  
<sup>4</sup>E.L. Nagaev, *Phys. Rep.* **346**, 387 (2001).  
<sup>5</sup>M.S. Salamon and M. Jaime, *Rev. Mod. Phys.* **73**, 583 (2001).  
<sup>6</sup>T.W. Darling, A. Migliori, E.G. Moshopoulou, S.A. Trugman, J.J. Neumeier, J.L. Sarrao, A.R. Bishop, and J.D. Thompson, *Phys. Rev. B* **57**, 5093 (1998).  
<sup>7</sup>Y.P. Gaidukov, N.P. Danilova, A.A. Mukhin, and A.M. Balbashov, *Pis'ma Zh. Éksp. Teor. Fiz.* **68**, 141 (1998) [*JETP Lett.* **68**, 153 (1998)].  
<sup>8</sup>Changfei Zhu and Renkui Zheng, *Phys. Rev. B* **59**, 11169 (1999).  
<sup>9</sup>R.I. Zainullina, N.G. Bebenin, V.V. Mashkautsan, A.M. Burkhanov, Y.P. Sukhorukov, V.V. Ustinov, V.G. Vassiliev, and B.V. Slobodin, *Fiz. Tverd. Tela. (St. Petersburg)* **42**, 284 (2000) [*Phys. Solid State* **42**, 292 (2000)].  
<sup>10</sup>H. Hazama, T. Goto, Y. Nemoto, Y. Tomioka, A. Asamitsu, and Y. Tokura, *Phys. Rev. B* **62**, 15 012 (2000).  
<sup>11</sup>K.G. Bogdanova, A.R. Bulatov, V.A. Golenishchev-Kutuzov, and M.M. Shakirzyanov, *Fiz. Tverd. Tela. (St. Petersburg)* **43**, 1512 (2001) [*Phys. Solid State* **43**, 1572 (2001)].  
<sup>12</sup>R.I. Zainullina, N.G. Bebenin, V.V. Mashkautsan, A.M. Burkhanov, V.S. Gaviko, V.V. Ustinov, Y.M. Mukovskii, D.A. Shulyatev, and V.G. Vassiliev, *Zh. Éksp. Teor. Fiz.* **120**, 139 (2001) [*JETP* **93**, 121 (2001)].  
<sup>13</sup>R.I. Zainullina, N.G. Bebenin, A.M. Burkhanov, V.V. Ustinov, Y.M. Mukovskii, A.A. Arsenov, *Pis'ma Zh. Éksp. Teor. Fiz.* **74**, 120 (2001) [*JETP Lett.* **74**, 115 (2001)].  
<sup>14</sup>A. Urushibara, Y. Morimoto, T. Arima, A. Asamitsu, G. Kido, and Y. Tokura, *Phys. Rev. B* **51**, 14103 (1995).  
<sup>15</sup>H. Kawano, R. Kajimoto, and H. Yoshizawa, *Phys. Rev. B* **53**, R14 709 (1996).  
<sup>16</sup>Y. Yamada, O. Hino, S. Nohdo, R. Kanao, T. Inami, and S. Katano, *Phys. Rev. Lett.* **77**, 904 (1996).  
<sup>17</sup>D. Shulyatev, S. Karabashev, A. Arsenov, and Ya. Mukovskii, *J. Cryst. Growth* **198/199**, 511 (1999).  
<sup>18</sup>H.J. McSkimin, in *Physical Acoustics. Principles and Methods*, edited by W.P. Mason (Academic Press, New York, 1964), Vol. I, Part A, p. 272.  
<sup>19</sup>L.D. Landau and E.M. Lifshitz, *Theory of Elasticity*, 2nd ed. (Pergamon, London, 1970).  
<sup>20</sup>L. Vasiliu-Doloc, J.W. Lynn, A.H. Moudden, A.M. de Leon Guevara, and A. Revcolevschi, *Phys. Rev. B* **58**, 14913 (1998).  
<sup>21</sup>D.H. Niblett, in *Physical Acoustics. Principles and Methods*, edited by W.P. Mason (Academic Press, New York 1966), Vol. III, Part A, p. 78.  
<sup>22</sup>C. Wert, in *Physical Acoustics. Principles and Methods*, (Ref. 21), Vol. III, Part A, p. 44.  
<sup>23</sup>N.N. Loshkareva, Y.P. Sukhorukov, E.A. Neifeld, V.E. Arkhipov, A.V. Korolev, V.S. Gaviko, E.A. Panfilova, Y.M. Mukovskii, and D.A. Shulyatev, *Zh. Éksp. Teor. Fiz.* **117**, 440 (2000) [*JETP* **90**, 389 (2000)].